Electron Propagator Theory of the Photoelectron Spectrum of Methanesulfenic Acid

J. V. Ortiz*

Department of Chemistry, Kansas State University, Manhattan, Kansas 66506-3701

Received: August 23, 2000

Assignment of the photoelectron spectrum of methanesulfenic acid, H_3CSOH, is facilitated by ab initio electron propagator calculations. Close agreement exists between experimental peak positions and predictions at the NR2 level of theory for the first three ionization energies. A fourth state, which may be obscured by impurities generated in the thermolytic synthesis of evanescent H_3CSOH molecules, is predicted. A nearby correlation state has also been discovered. Two higher ionization energies predicted by NR2 theory are in close agreement with a feature identified in the spectrum. Finally, a previously unassigned peak at higher energy has been explained on the basis of the NR2 calculations. Dyson orbitals corresponding to each ionization energy are analyzed in terms of their uncorrelated, Hartree−Fock counterparts and their atomic constituents.

Introduction

Interest in electronic structure and bonding in sulfenic acids is motivated by the rich patterns of reactivity of these compounds in organic,[1] protein,[2] and atmospheric[3] chemistry. They are implicated as intermediates in the chemistry of freshly cut *Allium savitum* (garlic) and *Allium cepa* (onion).[4] Their importance in the photochemical degradation of methane thiol and dimethyl sulfoxide[3] has stimulated extensive investigation of the gas-phase ion chemistry of methanesulfenic acid, H_3CSOH.[5] Sulfenic acid molecules readily react with each other to produce thiosulfinates, and their characterization therefore is challenging. Extensive synthetic efforts have been expended on the preparation of stable, isolable sulfenic acids with bulky substituents.[6,7] Evanescent H_3CSOH molecules were studied with microwave spectroscopy[8] and then by mass spectrometry.[5,9] Compounds with longer alkyl chains or aryl substituents have been examined with matrix−infrared spectroscopy.[10,11]

To investigate the electronic structure of methanesulfenic acid, Lacombe and co-workers undertook a photoelectron study of the flash−vacuum thermolysis of two known precursors of this molecule.[12] They succeeded in showing the advent of additional spectral features with increasing temperature. Peaks found with both precursors were assigned to ionization energies (IEs) of H_3CSOH. To facilitate assignment of the spectral features, ab initio and semiempirical calculations were performed. Koopmans's theorem (KT) results predicted that the molecular orbital (MO) corresponding to the lowest IE consists chiefly of nonbonding p functions on S that have only weak π interactions with the methyl group. Convincing evidence for this characterization was provided by the decrease in relative intensity of the lowest IE feature accompanying the use of He II instead of He I radiation. For the following orbital, some localization on S remained, but delocalization onto O was also important. Semiempirical KT predictions were in closer agreement with the experimental peaks than their ab initio counterparts. Correlated calculations using second-order total energies and a variational−perturbative technique confirmed these interpretations for the two lowest IEs. Four peaks, obtained after subtraction of features corresponding to impurities, were assigned.

* E-mail: ortiz@ksu.edu.

Computational investigations have established the relative stability of the H_3CSOH isomer with respect to the sulfoxide form, H_3COSH.[13] Geometry optimizations at the MP2/6−31G* level[12] confirm conclusions based on microwave spectroscopy[8] in which the favored gauche conformation has a C−S−O−H dihedral angle near 90°. QCISD(T) calculations of the lowest vertical IE of methanesulfenic acid[14] are in close agreement with the photoelectron spectrum (PES) result.[12] The absence of point group symmetry in H_3COSH has impeded computational examination of higher IEs with methods designed chiefly for ground states of a given irreducible representation.

Only KT results are available for higher IEs. This level of theory asserts that holes corresponding to the third and fourth states have σ bonding character. According to ref 12, localization on S−O and C−H bonds occurs in the former and on C−S and C−H bonds in the latter.

Here, the PES of H_3COSH are investigated with correlated, ab initio electron propagator methods.[15−20] With these techniques, it is possible to calculate correlation corrections to the results of KT in a systematic manner. In addition, to each IE there corresponds a Dyson orbital, ψ^{Dyson}, which represents the overlap between the initial, N-electron state, Ψ_N, and the final state with $N - 1$ electrons, Ψ_{N-1}. Dyson orbitals are defined by

$$\psi^{\mathrm{Dyson}}(x_1) = \int \Psi_N(x_1,x_2,x_3,...,x_N)\Psi^*_{N-1}(x_2,x_3,x_4,...,x_N)dx_2dx_3dx_4...dx_N \quad (1)$$

where x_i is the space−spin coordinate of electron i. The norm of the Dyson orbital is known as the pole strength, p, and is given by

$$p = \int |\psi^{\mathrm{Dyson}}(x_1)|^2 dx_1 \quad (2)$$

When electron correlation and final state orbital relaxation are neglected (as in KT), Dyson orbitals equal canonical, Hartree−Fock orbitals and pole strengths equal unity. For high photoelectron energies, photoionization intensities are proportional to pole strengths and to squares of transition operator matrix elements between Dyson and continuum orbitals. When main ionization peaks and their satellites are assumed to have

10.1021/jp0030342 CCC: $19.00
Published on Web 11/08/2000

TABLE 1: Optimized Geometry

bond length	Å	bond angle	°	dihedral angle	°
S—C	1.791				
O—S	1.688	O—S—C	99.6		
H—O	0.962	H—O—S	106.0	H—O—S—C	90.8
H_1—C	1.091	H_1—C—S	110.4	H_1—C—S—O	56.6
H_2—C	1.094	H_2—C—S	106.5	H_2—C—S—O	174.6
H_3—C	1.092	H_3—C—S	112.1	H_3—C—S—O	−66.5

TABLE 2: Ionization Energies (eV) and Pole Strengths

number	attribution[12]	PES[12]	NR2	p	KT
1	$n_S^{\perp}$	9.01	8.80	0.90	9.54
2	n_S, n_O, σ_{CS}	11.08	10.86	0.89	12.06
3	σ_{CH}, n_O	12.92	12.92	0.87	14.41
4	σ_{CH}, σ_{CS}, σ_{SO}	14.0[1]	14.03[a]	0.84	15.70
4a			14.51	0.03	
5	σ_{CH}, n_O	14.95	14.82	0.88	16.15
6	σ_{CH}, n_O	14.95	15.17	0.87	16.54
7	σ_{OH}		16.59	0.79	18.50

[a] This estimate is necessitated by the presence of other molecules.

Dyson orbitals that are proportional to a single, Hartree−Fock orbital and when the corresponding matrix elements with continuum orbitals are assumed to be equal, intensity ratios are proportional to pole strengths. Electron propagator calculations provide direct determinations of IEs, Dyson orbitals, and pole strengths without evaluation of the many electron wave functions of the initial or final states.

Methods

The NR2 electron propagator approximation[21] is used. This method has provided accurate accounts of the outer valence PES of closed-shell molecules, with an average absolute error of approximately 0.15 eV when a basis set of triple ζ quality or better is used. The 6−311G(2df,2pd) basis[22] is used in the NR2 calculations. IEs are converged to within 0.01 millihartree. Core orbitals are omitted from summations that are performed in the NR2 calculations.

The geometry of the H_3CSOH molecule is optimized at the MP2/6−311G(d,p) level. The initial guess structure is taken from MP2/6−31+G(d) data in the PES report.[12] In addition, structures with C_s symmetry are optimized.

Energy minimizations are performed with Gaussian 98.[23] Electron propagator calculations are executed with a link connected to this program.

Plots of orbitals are produced with MOLDEN.[24]

Results

Geometry optimization yields a structure (see Table 1) that closely resembles its antecedents in the literature.[12−14] The H—O—S—C dihedral angle of 90.8° eliminates the relevance of structures with planes of symmetry. C_s symmetry may be imposed by fixing this dihedral at 0° or 180° and by considering pairs of rotamers where the methyl group has two protons linked by a reflection plane. All four of these structures are less stable than the optimized C_1 geometry by at least 4.7 kcal/mol and therefore are ignored henceforth.

IEs and pole strengths in the NR2 approximation are tabulated in Table 2. Four IEs assigned on the basis of the PES[12] and KT results obtained with the 6−311G(2df,2pd) basis are listed as well.

For each IE with index r, the corresponding Dyson orbital has been normalized to unity and subsequently expressed as a linear combination of noncore, canonical, Hartree−Fock (HF) orbitals with index q that runs over occupied and virtual orbitals:

$$\psi_r^{\text{Dyson}} = p_r^{-1/2}\psi_r^{\text{Dyson}} = \sum_q C_{qr}\phi_q^{\text{HF}}. \quad (3)$$

(In the Koopmans approximation, $p = 1$ and all C coefficients except one are zero.) C coefficients whose absolute values exceed 0.1 are shown in Table 3. For all of the Dyson orbitals, except that of the lowest IE, there are significant mixings between the Koopmans component and other canonical, HF orbitals.

For each IE with index r calculated in the NR2 approximation, there is an ionization operator, O_r, whose effect on the initial, N-electron state is to produce an ionized state with index r and $N-1$ electrons. This ionization operator is a linear combination of simple electron annihilation operators (a) and of products of one electron creation operator ($a^{\dagger}$) and two electron annihilation operators:

$$O_r = \sum_i^{\text{occupied}} a_i c_{i,r} + \sum_b^{\text{virtual}} a_b c_{b,r} + \sum_{i<j}^{\text{occupied}} \sum_b^{\text{virtual}} a_b^{\dagger} a_i a_j c_{ijb,r} + \sum_{b<c}^{\text{virtual}} \sum_i^{\text{occupied}} a_i^{\dagger} a_b a_c c_{bci,r} \quad (4)$$

The summation indices refer to occupied or virtual spin orbitals. If the vector of operator coefficients, $\mathbf{c}_r$, is normalized such that

$$\mathbf{c}_r^{\dagger}\mathbf{c}_r \equiv \sum_i^{\text{occupied}} |c_{i,r}|^2 + \sum_b^{\text{virtual}} |c_{b,r}|^2 + \sum_{i<j}^{\text{occupied}} \sum_b^{\text{virtual}} |c_{ijb,r}|^2 + \sum_{b<c}^{\text{virtual}} \sum_i^{\text{occupied}} |c_{bci,r}|^2 = 1, \quad (5)$$

then the pole strength reads

$$p_r = \sum_i^{\text{occupied}} |c_{i,r}|^2 + \sum_b^{\text{virtual}} |c_{b,r}|^2. \quad (6)$$

The coefficients of the normalized Dyson orbital and the coefficients of the simple annihilation operators are related by

$$C_{ir} = p_r^{-1/2} c_{i,r} \quad (7)$$

and

$$C_{br} = p_r^{-1/2} c_{b,r}. \quad (8)$$

Measures of the importance of orbital relaxation and electron correlation are provided by comparisons with the IEs, Dyson orbitals, pole strengths, and ionization operators implicit in the Koopmans picture of electronic structure. In this uncorrelated, frozen-orbital limit, IEs equal occupied, canonical HF orbital energies, Dyson orbitals are identical to canonical HF orbitals, pole strengths are unity, and ionization operators have only one component corresponding to a single, simple annihilation operator (that is, all c coefficients vanish save one).

For the cationic states of greatest interest here, the ionization operators, O_r, are dominated by simple annihilation operators with occupied orbital indices. In some cases, there are also significant contributions from two-hole, one-particle (2hp) ionization operators. Coefficients ($c_{ijb,r}$) of these 2hp operators ($a_b^{\dagger}a_i a_j$) with absolute values greater than 0.1 are listed in Table 4. For three cationic states, contributions of this magnitude appear.

TABLE 3: Dyson Orbitals

Dyson orbital	combination of HF orbitals
1	$1.00\ \phi_{HOMO}$
2	$0.97\ \phi_{HOMO-1} + 0.16\ \phi_{HOMO-2} - 0.14\ \phi_{HOMO-3} + 0.10\ \phi_{HOMO-4}$
3	$0.95\ \phi_{HOMO-2} - 0.21\ \phi_{HOMO-1} - 0.11\ \phi_{HOMO-3} + 0.15\ \phi_{HOMO-4} - 0.13\ \phi_{HOMO-5}$
4	$0.94\ \phi_{HOMO-3} + 0.13\ \phi_{HOMO-1} + 0.18\ \phi_{HOMO-2} - 0.23\ \phi_{HOMO-4} - 0.13\ \phi_{HOMO-6}$
4a	$0.86\ \phi_{HOMO-3} + 0.11\ \phi_{LUMO} + 0.11\ \phi_{HOMO} + 0.28\ \phi_{HOMO-1} - 0.13\ \phi_{HOMO-2} - 0.25\ \phi_{HOMO-6} + 0.24\ \phi_{HOMO-7}$
5	$0.93\ \phi_{HOMO-4} - 0.16\ \phi_{HOMO-2} + 0.26\ \phi_{HOMO-3} - 0.18\ \phi_{HOMO-5}$
6	$0.95\ \phi_{HOMO-5} + 0.13\ \phi_{HOMO-2} + 0.23\ \phi_{HOMO-4} + 0.13\ \phi_{HOMO-6}$
7	$0.97\ \phi_{HOMO-6} + 0.14\ \phi_{HOMO-3} - 0.16\ \phi_{HOMO-5} + 0.11\ \phi_{HOMO-7}$

TABLE 4: Shakeup Operators

state	operator	coefficient
4	$a^{\dagger}_{LUMO\beta}\ a_{HOMO\alpha}\ a_{HOMO\beta}$	0.13
4a	$a^{\dagger}_{LUMO\beta}\ a_{HOMO\alpha}\ a_{HOMO\beta}$	0.74
	$a^{\dagger}_{LUMO+2\beta}\ a_{HOMO\alpha}\ a_{HOMO\beta}$	−0.11
	$a^{\dagger}_{LUMO+3\beta}\ a_{HOMO\alpha}\ a_{HOMO\beta}$	−0.26
	$a^{\dagger}_{LUMO+4\beta}\ a_{HOMO\alpha}\ a_{HOMO\beta}$	0.20
	$a^{\dagger}_{LUMO+5\beta}\ a_{HOMO\alpha}\ a_{HOMO\beta}$	−0.14
	$a^{\dagger}_{LUMO+8\beta}\ a_{HOMO\alpha}\ a_{HOMO\beta}$	0.38
7	$a^{\dagger}_{LUMO+2\beta}\ a_{HOMO\alpha}\ a_{HOMO\beta}$	0.14
	$a^{\dagger}_{LUMO+7\beta}\ a_{HOMO\alpha}\ a_{HOMO\beta}$	0.12

Contours have been plotted for the seven highest occupied MOs (Figures 1−7) and for the lowest unoccupied MO or lowest unoccupied molecular orbital (LUMO) (Figure 8).

Discussion

NR2 and experiment agree closely for the first IE assigned in ref 12. Corrections to KT results are large, but the pole strength is typical for outer valence IEs of closed-shell molecules. Additional improvements to the basis can be expected to increase the NR2 result by approximately 0.1 eV and thus improve agreement even further.[25] QCISD(T) calculations[26] with a larger basis produce an IE of 9.04 eV.[28] In ref 12, ΔMP2[27] and CIPSI[28] calculations with the 6−311(d,p) basis yield 8.86 and 8.92 eV, respectively.

Figure 1 shows the highest occupied MO (HOMO). According to Table 3, the HOMO is practically identical to the Dyson orbital. A narrow feature in the PES for the first IE corresponds to a Dyson orbital that is dominated by p functions on S. Delocalization into the methyl group via π interactions is minor; an antibonding relationship with a p function on O is more prominent. Diminished relative intensity for this peak with He II versus He I radiation is compatible with localization on S.

For the second IE, the proximity similar between experiment and NR2 results. CIPSI calculations from ref 12 produced a value in reasonable agreement with experiment: 10.65 eV. (CIPSI results for the two lowest cationic states only were reported.) Corrections to KT results are larger than for the first IE, although the pole strength is still approximately 0.9.

Another narrow peak in the PES maps onto a Dyson orbital whose dominant component, ϕ_{HOMO-1} (see Figure 2), has nonbonding S and O lobes with opposing phases. Because He I and He II relative intensities for this state are approximately equal, localization on S is expected to be less pronounced for this Dyson orbital. A large lobe occurs in the C−S bond region. As for the Dyson orbitals of all of the remaining IEs, there are significant mixings between the chief HF orbital component and other canonical orbitals.

C−H σ bonding character in the third Dyson orbital explains the greater width of the peak at 12.92 eV. Large O p contributions are present also in the dominant HF orbital, ϕ_{HOMO-2}. There is fortuitously close agreement between the NR2 prediction and the experimental assignment. It is likely that basis set improvements and a more detailed account of electron correlation would produce significant, but canceling corrections. Even larger corrections to KT results appear here and the pole strength is somewhat lower.

As thermolysis of the precursor methyl methanethiosulfinate gives rise to methanesulfenic acid and to thioformaldehyde, interference from an IE of the latter molecule at 13.85 eV[29] prevents assignment of features in this region of the spectrum. Use of another precursor, methyl *tert*-butyl sulfoxide, gives rise to features at 14.00, 14.94, and 16.80 eV after subtraction of the spectrum of the byproduct isobutene. The first two peaks are part of a broad, highly structured feature that extends from 14.0 to about 15.2 eV.

Four NR2 IEs at 14.03, 14.82, 15.17, and 16.59 eV correspond to these observations. Large corrections to KT results

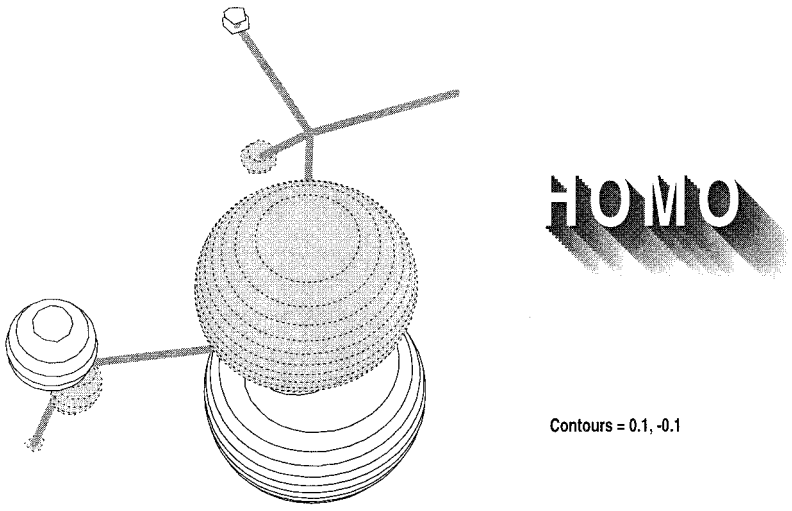

Figure 1. Hartree−Fock HOMO.

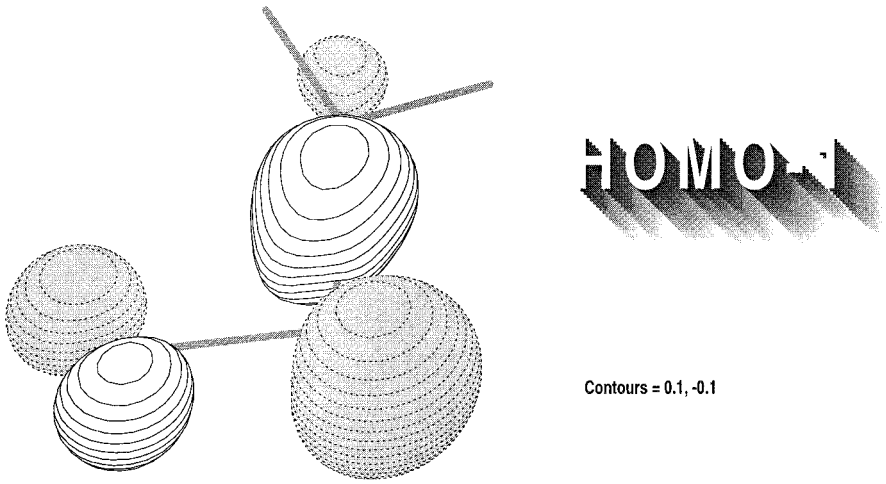

Figure 2. Hartree−Fock HOMO-1.

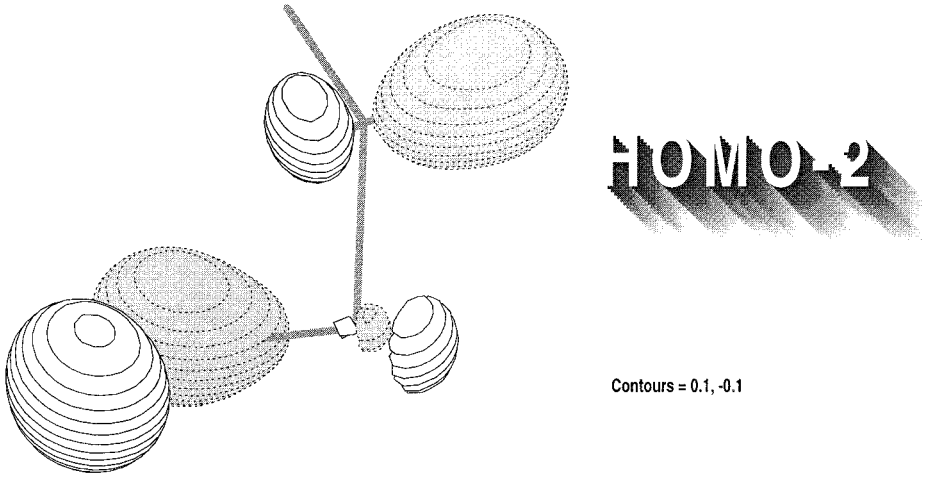

Figure 3. Hartree−Fock HOMO-2.

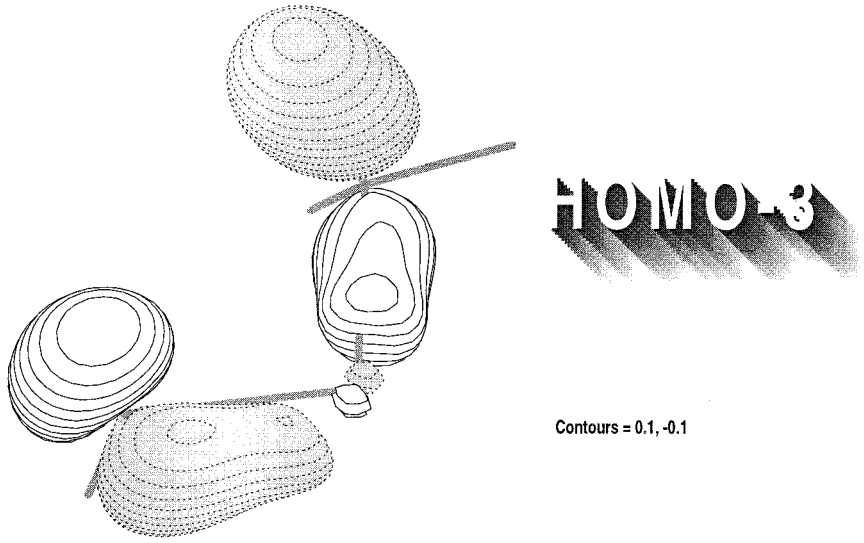

Figure 4. Hartree−Fock HOMO-3.

are found in all cases, which are numbered 4, 5, 6, and 7 in Tables 2 and 3. Pole strengths for the first three IEs vary between 0.84 and 0.88 and the Dyson orbitals exhibit significant mixings. For states 4 and 7, there are 2hp operators with noteworthy coefficients. For each 2hp operator displayed in Table 4, two electrons are removed from the HOMO and a single electron is created in a low-lying, unoccupied orbital.

$\phi_{\mathrm{HOMO-3}}$, the dominant HF contributor to the fourth Dyson orbital, exhibits bonding C—S, C—H, and O—S relationships in Figure 4. (Note the small lobes near the S nucleus that disclose the positions of 3p radial nodes.) In the PES of an isolated molecule, this IE can be expected to pertain to a wide peak with underlying vibrational structure.

A table in ref 12 places the experimental IE at 14.95 eV on

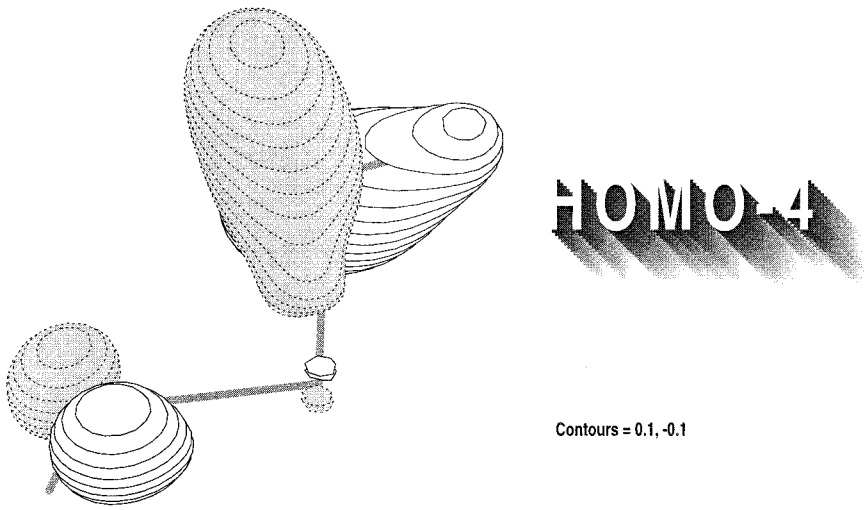

Figure 5. Hartree−Fock HOMO-4.

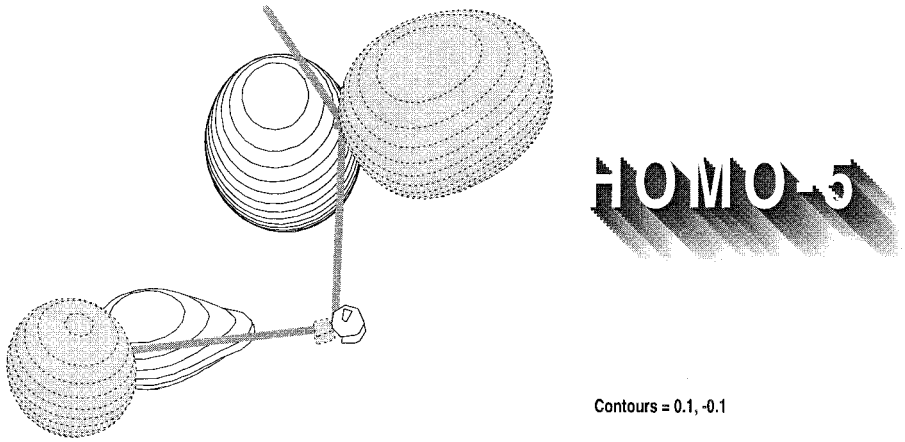

Figure 6. Hartree−Fock HOMO-5.

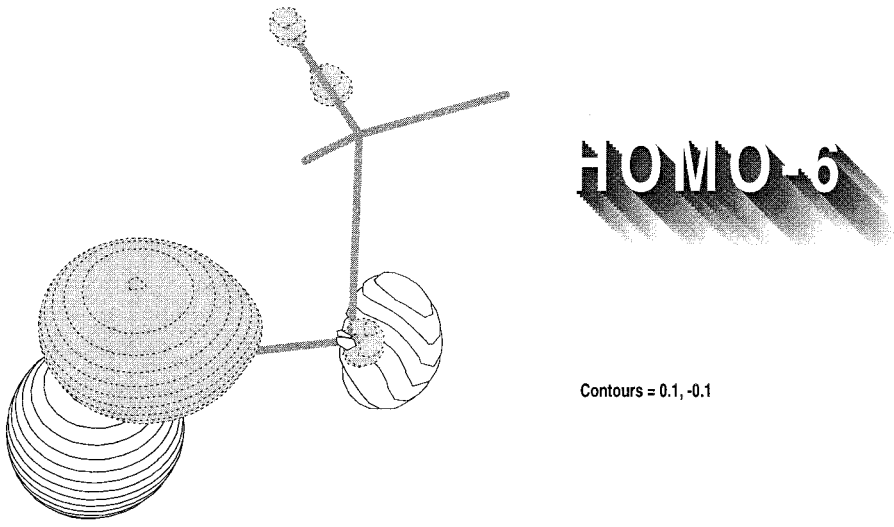

Figure 7. Hartree−Fock HOMO-6.

the same line with the fourth highest occupied orbital energy. On the basis of the present calculations, this broad feature should be assigned to the fifth and sixth highest occupied MOs. In the corresponding HF orbitals in Figures 5 and 6, C−H bonding lobes mix with nonbonding O 2p functions.

The last feature discerned through PES at 16.80 may be assigned to IE number 7, which has a markedly lower pole strength, 0.79. Constructive interference between H and O functions is important in the orbital displayed in Figure 7.

In the course of searching for NR2 IEs with large pole strengths, another state, labeled 4a in Tables 2−4, was discovered. This state has no KT counterpart, for its ionization operator is dominated by 2hp components, especially the $a^{\dagger}_{\mathrm{LUMO}\beta}\, a_{\mathrm{HOMO}\alpha} a_{\mathrm{HOMO}\beta}$ operator. A low pole strength, 0.03,

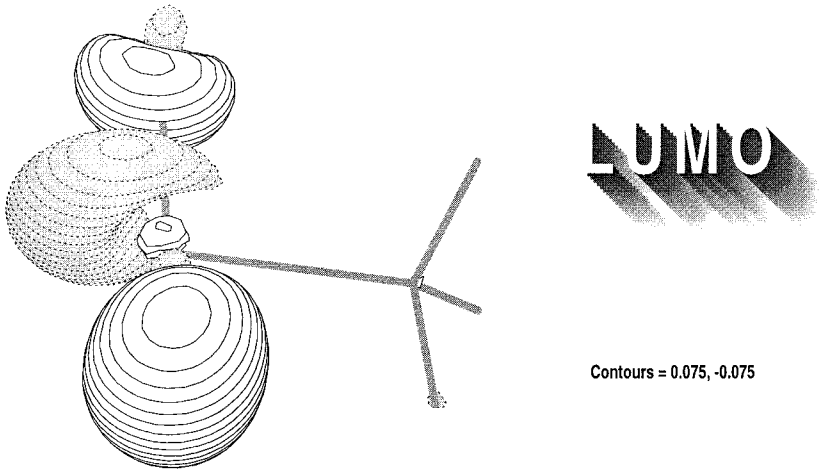

Figure 8. Hartree−Fock LUMO.

marks 4a as a correlation state. In the corresponding Dyson orbital, the third highest occupied MO makes the largest contribution. This state occurs between the more Koopmans-like final states at 14.03 and 14.82 eV in NR2 calculations. In a simple orbital picture, two electrons are removed from the nonbonding HOMO and a single electron is deposited in the LUMO. The latter orbital, shown in Figure 8, has an antibonding interference pattern between S and O. Considerable mixing with d functions distorts the S 3p lobes. Because the Dyson orbital is dominated by $\phi_{\mathrm{HOMO-3}}$, the relative intensities of the 4 and 4a states should be approximately equal to the ratio of their respective pole strengths.

Conclusions

An assignment of the He I and He II PES of methanesulfenic acid has been effected on the basis of ab initio electron propagator calculations in the NR2 approximation. Agreement within 0.2 eV of experiment has been achieved for the first three IEs. Sulfur p functions dominate the Dyson orbital of the first IE. Nonbonding S and O lobes with opposite phases and C−S bonding interactions dominate the Dyson orbital of the second IE. C−H σ bonding in the third Dyson orbital corresponds to a broader peak in the PES. A feature at 14.00 eV has been assigned to the fourth IE; the corresponding Dyson orbital has C−H, C−S, and S−O bonding character. A correlation final state with two holes in the HOMO and an electron in the LUMO is predicted at 14.5 eV. Two cationic states underlie the feature seen at 14.95 in the PES and both Dyson orbitals possess C−H bonding and O nonbonding lobes. In addition, another peak seen at 16.80 eV has been assigned; its Dyson orbital displays O−H bonding character.

Acknowledgment. O. Dolgounitcheva and V. G. Zakrzewski of Kansas State University provided essential technical support. This work was supported by the National Science Foundation under grant CHE-9873897 and by Gaussian, Incorporated.

References and Notes

(1) Patai, S., Ed.; *The chemistry of sulphenic acids and derivatives*, J. Wiley and Sons: Chichester, 1990.
(2) Allison, W. S. *Acc. Chem. Res.* **1976**, *9*, 293.
(3) Graedel, T. E. *Rev. Geophys. Space Phys.* **1977**, *15*, 421.
(4) Block, E. *Angew. Chem., Int. Ed. Engl.* **1992**, *31*, 1135.
(5) Turecek, F.; Drinkwater, D. E.; McLafferty, F. W. *J. Am. Chem. Soc.* **1994**, *111*, 7696.
(6) Ishii, A.; Komiya, K.; Nakayama, J. *J. Am. Chem. Soc.* **1996**, *118*, 12836.
(7) Goto, K.; Holler, M.; Okazaki, R. *J. Am. Chem. Soc.* **1997**, *119*, 1460.
(8) Penn, R. E.; Block, E.; Revelle, L. *J. Am. Chem. Soc.* **1978**, *100*, 3622.
(9) Turecek, F.; Brabec, L.; Vondrak, T.; Hanus, V.; Hajicek, J.; Havlas, Z. *Collect. Czech. Chem. Commun.* **1988**, *53*, 2140.
(10) Davis, F. A.; Billmers, R. L. *J. Org. Chem. Soc.* **1985**, *50*, 2593.
(11) Barret, G. C. In *The Chemistry of Sulphenic Acids and Derivatives*; Patai, S., Ed.; J. Wiley and Sons: Chichester, 1990; p 1.
(12) Lacombe, S.; Loudet, M.; Banchereau, E.; Simon, M.; Pfister-Guillouzo, G. *J. Am. Chem. Soc.* **1996**, *118*, 1131.
(13) Toz, T.; Basch, H. In *Supplement S: The Chemistry of Sulfur-Containing Functional Groups*; Patai, S., Rapaport, Z., Eds.; J. Wiley and Sons: New York, 1993; p 1.
(14) Turecek, F. *J. Phys. Chem.* **1994**, *98*, 3701.
(15) Linderberg, J.; Öhrn, Y. *Propagators in Quantum Chemistry*; Academic Press: New York, 1973.
(16) Ortiz, J. V. In *Computational Chemistry: Reviews of Current Trends*; Leszczynski, J., Ed.; World Scientific: Singapore, 1997; Vol. 2, p 1.
(17) Ortiz, J. V. In *Conceptual Perspectives in Quantum Chemistry*; Calais, J.-L., Kryachko, E., Eds.; Kluwer: Dordrecht, 1997; Vol. 3, p 465.
(18) Ortiz, J. V. *Adv. Quantum Chem.* **1999**, *35*, 33.
(19) von Niessen, W.; Schirmer, J.; Cederbaum, L. S. *Comput. Phys. Rep.* **1984**, *1*, 57.
(20) Simons, J. In *Theoretical Chemistry: Advances and Perspectives*; Eyring, H., Henderson, D., Eds.; Academic Press: New York, 1978; Vol. 3, p 1.
(21) Ortiz, J. V. *J. Chem. Phys.* **1998**, *108*, 1008.
(22) Krishnan, R.; Binkley, J. S.; Seeger, R.; Pople, J. A. *J. Chem. Phys.* **1980**, *72*, 650. McLean, A. D.; Chandler, G. S. *J. Chem. Phys.* **1980**, *72*, 5639. Francl, M. M.; Pietro, W. J.; Hehre, W. J.; Binkley, J. S.; Gordon, M. S.; DeFrees, D. J.; Pople, J. A. *J. Chem. Phys.* **1982**, *77*, 3654. Frisch, M. J.; Pople, J. A.; Binkley, J. S. *J. Chem. Phys.* **1984**, *80*, 3265.
(23) Frisch, M. J.; Trucks, G. W.; Schlegel, H. B.; Scuseria, G. E.; Robb, M. A.; Cheeseman, J. R.; Zakrzewski, V. G.; Montgomery, Jr., J. A.; Stratmann, R. E.; Burant, J. C.; Dapprich, S.; Millam, J. M.; Daniels, A. D.; Kudin, K. N.; Strain, M. C.; Farkas, O.; Tomasi, J.; Barone, V.; Cossi, M.; Cammi, R.; Mennucci, B.; Pomelli, C.; Adamo, C.; Clifford, S.; Ochterski, J.; Peterson, G. A.; Ayala, P. Y.; Cui, Q.; Morokuma, K.; Malick, D. K.; Rabuck, A. D.; Raghavachari, K.; Foresman, J. B.; Cioslowski, J.; Ortiz, J. V.; Stefanov, B. B.; Liu, G.; Liashenko, A.; Piskorz, P.; Komaromi, I.; Gomperts, R.; Martin, R. L.; Fox, D. J.; Keith, T.; Al-Laham, M. A.; Peng, C. Y.; Nanayakkara, A.; Gonzalez, C.; Challacombe, M.; Gill, P. M. W.; Johnson, B.; Chen, W.; Wong, M. W.; Andres, J. L.; Head-Gordon, M.; Replogle, E. S.; Pople, J. A. *GAUSSIAN 98* (Revision A8); Gaussian, Inc.: Pittsburgh, PA, 1998.
(24) Schaftenaar, G. *MOLDEN 3.4*; CAOS/CAMM Center: The Netherlands, 1998.
(25) Partial results with the 6-311G(3d2f, 2p) basis, for example, produce IEs of 8.84, 10.91, 12.96, 14.06, 14.46, and 14.81 eV for states 1−4, 4a, and 5, respectively.
(26) Pople, J. A.; Head-Gordon, M.; Raghavachari, K. *J. Chem. Phys.* **1987**, *87*, 5968.
(27) Bartlett, R. J. *Annu. Rev. Phys. Chem.* **1981**, *32*, 359.
(28) Huron, B.; Malrieu, J. P.; Rancurel, P. *J. Chem. Phys.* **1973**, *58*, 5745.
(29) Solouki, B.; Rosmus, P.; Bock, H. *J. Am. Chem. Soc.* **1976**, *98*, 6054.